

LeanQuant: Accurate Large Language Model Quantization with Loss-Error-Aware Grid

Tianyi Zhang¹, Anshumali Shrivastava^{1,2}

¹Department of Computer Science, Rice University, ²ThirdAI Corp.
{tz21, anshumali}@rice.edu

Abstract

Large language models (LLMs) have numerous applications across various domains, but their high computational and memory demands pose significant deployment challenges. Weight quantization is an effective technique for reducing the decoding latency and memory requirements of LLMs. Existing approaches primarily aim to maintain the quality of quantized models by preserving outliers in input features, but they still suffer significant quality loss at lower bit widths. Our approach builds on Optimal Brain Quantization (OBQ), an iterative weight-update-based quantization framework. We identify a key limitation of OBQ, specifically that its uniform quantization grid is sub-optimal for maintaining model quality, as it introduces large errors to the task loss. To address this, we propose LeanQuant, which learns a loss-error-aware quantization grid by leveraging the inverse diagonal Hessian. Extensive empirical evaluations demonstrate that LeanQuant is both efficient and accurate; it can quantize a 70-billion-parameter model in 6 hours using a single 32GB GPU and performs favorably compared to competitive baselines in the 4-bit, 3-bit, and 2-bit regions.

1 Introduction

Large language models (LLMs) have demonstrated impressive reasoning (Wei et al., 2022) and problem-solving abilities (Kojima et al., 2022), and shown the potential for bringing transformative changes to various fields such as law (Kaddour et al., 2023) and education (Kasneci et al., 2023). However, deploying LLMs in a cost-effective manner presents significant challenges due to their substantial memory and computational demands (Chen et al., 2023). Efficient inference with LLMs requires dedicated hardware accelerators, such as GPUs with high memory capacity. This requirement significantly hinders the accessibility and democratization of artificial intelligence (Kaddour

et al., 2023).

Weight quantization (Krishnamoorthi, 2018) is a technique that stores the floating-point model parameters as low-bit-width integers at a reduced precision, and it can effectively reduce the memory footprint and decoding latency of LLMs (Frantar et al., 2022). For instance, the weights of the LLaMA-2-70b model (Touvron et al., 2023b) occupy approximately 140GB of GPU memory, which would require at least two A100-80GB GPUs for inference. However, when the model is quantized to 2 bits per weight, the size of model weights drops to around 18GB, enabling it to run on a single off-the-shelf RTX 4090 24GB GPU without costly inter-GPU communication.

After quantization, the original floating-point weight is represented compactly by the index of the nearest grid line in the quantization grid. This saves memory but comes at the cost of precision loss of weights, which can lead to catastrophic model quality degradation. Previously works have identified the emergence of outlier input features in LLMs (Dettmers et al., 2022), and found that preserving them is critical for maintaining model quality. To preserve the salient weights, existing methods leverage mixed-precision decomposition (Dettmers et al., 2022), difficulty migration (Xiao et al., 2023), or activation-aware channel scaling (Lin et al., 2024). OmniQuant (Shao et al., 2024) performs gradient descent to learn the optimal weight clipping and equivalent transformations to better preserve quantized precision. However, these approaches still suffer from considerable model quality degradation in lower bit widths.

A particularly promising direction in quantization is Optimal Brain Quantization (OBQ) (Frantar and Alistarh, 2022), an iterative framework on which GPTQ (Frantar et al., 2022) is based. OBQ aims to minimize task loss errors caused by weight perturbations during quantization. It achieves this by quantizing weights one at a time and updating

the remaining weights in each step to compensate for the introduced error. OBQ uses approximations to derive a closed-form solution for the optimal weight update. However, even with these updates, quantizing each weight introduces some irreducible error to the loss. Our insight is that the uniform quantization grid used by OBQ is sub-optimal for ensuring low loss errors. By examining the mathematical formulation of loss error, we found that preserving the precision of weights with high values of inverse diagonal Hessians is crucial for keeping loss errors low and maintaining model quality. Based on this insight, we propose Loss-Error-Aware Network Quantization, or LeanQuant. Extensive empirical evaluations show that LeanQuant compares favorably to competitive baselines in quantizing language models, both large and small, ranging from million-parameter BERT models (Devlin et al., 2018) to billion-parameter LLaMA models (Touvron et al., 2023a,b), and effectively accelerates inference.

2 Background

In this section, we introduce the relevant background for our proposal including uniform quantization and Optimal Brain Quantization (Frantar and Alistarh, 2022).

2.1 Uniform Quantization

Uniform quantization is a commonly used approach for quantizing weights of deep neural networks (Krishnamoorthi, 2018). In uniform quantization, the quantization grid lines are evenly spaced out between the minimum and maximum value of the dynamic range of the weights. Then, the weights are quantized to the nearest grid line. To improve the quantization precision, the dynamic range is often recorded for each row \mathbf{w} of the weight matrices separately. In b -bit asymmetric quantization, the weight w_i within a row \mathbf{w} is quantized to the nearest grid line as follows,

$$\text{quant}(w_i) = \left\lfloor \frac{w_i - Z}{S} \right\rfloor \cdot S + Z$$

with $Z = \min(\mathbf{w})$ and $S = \frac{\max(\mathbf{w}) - \min(\mathbf{w})}{2^b - 1}$

(1)

where $\min(\mathbf{w})$ and $\max(\mathbf{w})$ are the minimum and maximum value in the row \mathbf{w} , and $\lfloor \cdot \rfloor$ represents the rounding function and Z, S are the zero-point and scaling factor.

2.2 Optimal Brain Quantization

Optimal Brain Quantization (OBQ) (Frantar and Alistarh, 2022) is a framework for quantizing deep neural networks post-training, based on the seminal works by LeCun et al. (1989) and Hassibi et al. (1993). The aim of post-training quantization (PTQ) is to minimize the impact of weight perturbations introduced by quantization on the network’s task loss, without requiring additional finetuning. Let $\mathcal{L}(\mathbf{w}_{\mathcal{N}})$ be the task loss of a network \mathcal{N} evaluated at the weights $\mathbf{w}_{\mathcal{N}}$ (flattened to a vector). Then, the PTQ objective is to minimize the loss error ϵ , which is defined as

$$\epsilon = \mathcal{L}(\mathbf{w}_{\mathcal{N}} + \delta_{\mathcal{N}}) - \mathcal{L}(\mathbf{w}_{\mathcal{N}}) \quad (2)$$

where $\delta_{\mathcal{N}}$ is the weight perturbation introduced by quantization. The loss error ϵ can be approximated with a Taylor series (LeCun et al., 1989) as

$$\epsilon = \underbrace{\left(\frac{\partial \mathcal{L}}{\partial \mathbf{w}_{\mathcal{N}}} \right)^{\top} \delta_{\mathcal{N}}}_{\text{negligible}} + \frac{1}{2} \delta_{\mathcal{N}}^{\top} \frac{\partial^2 \mathcal{L}}{\partial \mathbf{w}_{\mathcal{N}}^2} \delta_{\mathcal{N}} + \underbrace{O(\|\delta_{\mathcal{N}}\|^3)}_{\text{negligible}} \quad (3)$$

where the first term is omitted due to $\frac{\partial \mathcal{L}}{\partial \mathbf{w}_{\mathcal{N}}} \approx \mathbf{0}$ in a converged network, and the third and higher terms can be ignored due to small norms. Computing the exact Hessian $\mathbf{H} = \frac{\partial^2 \mathcal{L}}{\partial \mathbf{w}_{\mathcal{N}}^2}$ in a deep network is difficult, hence OBQ leverages an approximation of loss error proposed by Nagel et al. (2020),

$$\mathbb{E}(\epsilon) \approx \sum_l \|\mathbf{W}^l \mathbf{X}^l - \hat{\mathbf{W}}^l \mathbf{X}^l\|_F^2 \quad (4)$$

where $\mathbf{X}^l, \mathbf{W}^l, \hat{\mathbf{W}}^l$ are the input matrix, weight matrix, and quantized weight matrix of the linear layer l . As a result, the PTQ objective can be decomposed into layer-wise independent convex problems,

$$\arg \min_{\hat{\mathbf{W}}} \|\mathbf{W}\mathbf{X} - \hat{\mathbf{W}}\mathbf{X}\|_F^2 \quad (5)$$

which can be further decomposed into row-wise independent problems, since Equation 5 can be written as a sum of squares over the rows of \mathbf{W} .

OBQ employs an iterative quantization approach, in which a single weight in a row \mathbf{w} is quantized in each step, and then the remaining not-yet-quantized weights in the same row are updated to compensate for the introduced error. Given the constraint that the parameter w_i , indexed by i in row \mathbf{w} , is being quantized, the optimal weight perturbation δ to the

remaining weights can be solved with the following Lagrangian,

$$L(\delta, \lambda) = \frac{1}{2} \delta^\top \mathbf{H} \delta + \lambda \left(\mathbf{e}_i^\top \delta - (\text{quant}(w_i) - w_i) \right) \quad (6)$$

where the Hessian $\mathbf{H} = 2\mathbf{X}\mathbf{X}^\top$ (from Equation 5) is computed on a small sample of input data and \mathbf{e}_i is the i -th standard basis vector. Solving Equation 6 yields the optimal weight perturbation δ_i and the resulting loss error ϵ_i after quantizing w_i ,

$$\delta_i = \frac{\text{quant}(w_i) - w_i}{\mathbf{H}_{i,i}^{-1}} \mathbf{H}_{:,i}^{-1} \quad (7)$$

$$\epsilon_i = \frac{1}{2} \frac{(\text{quant}(w_i) - w_i)^2}{\mathbf{H}_{i,i}^{-1}} \quad (8)$$

where $\mathbf{H}_{i,i}^{-1}$ and $\mathbf{H}_{:,i}^{-1}$ denotes the i -th diagonal entry and the i -th column of the inverse Hessian, respectively.

The loss error ϵ_i reflects the negative impact of quantizing parameter w_i on the model quality, and it is always a non-negative value. OBQ utilizes the loss error ϵ_i as a heuristic for greedy optimization. Specifically, in each iteration, OBQ computes ϵ for all weights in a row and greedily selects the i -th parameter with the minimum ϵ_i to quantize. Then, w_i is round to the nearest value on the quantization grid, and the remaining weights are updated via $\mathbf{w} \leftarrow \mathbf{w} - \delta_i$, and the updated inverse Hessian for the remaining weights, with the i -th row and column removed from \mathbf{H} , is computed as

$$\mathbf{H}_{-i,-i}^{-1} = \left(\mathbf{H}^{-1} - \frac{\mathbf{H}_{:,i}^{-1} \mathbf{H}_{i,:}^{-1}}{\mathbf{H}_{i,i}^{-1}} \right)_{-i,-i} \quad (9)$$

This iterative process continues until all weights are quantized.

2.3 Scaling OBQ to Billion-Parameter LLMs

OBQ produces accurate post-training quantized models for million-parameter networks, but fails to scale to billion-parameter LLMs due to two primary reasons: the inefficient time complexity and the accumulation of numerical inaccuracies during updates. To improve its computational efficiency, Frantar et al. (2022) propose to quantize the weights in a fixed non-greedy order for all rows, and keep the weight updates within a block of B columns at a time. To prevent model quality collapse resulted from the accumulation of numerical inaccuracies by repeated weight updates, Frantar et al. (2022) propose to apply a mild damping ($\frac{1}{100}$

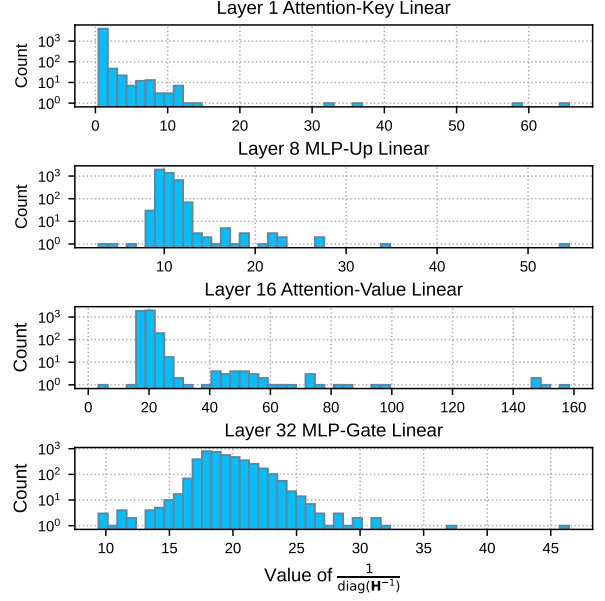


Figure 1: The empirical distributions of inverse diagonal Hessians, computed on 262K tokens from the C4 dataset for the LLaMA-2-7b model. Each layer has a few outlier values that significantly affect the overall loss error during the iterative quantization process.

of the average diagonals) to the diagonal entries of the Hessian \mathbf{H} and leverage a Cholesky decomposition of the inverse Hessian \mathbf{H}^{-1} in place of the update in Equation 9. The resulting algorithm is GPTQ, which quantizes billion-parameter LLMs efficiently and accurately.

3 Method

In this section, we introduce our proposed approach Loss-Error-Aware Network Quantization (Lean-Quant), which is able to quantize language models accurately and efficiently.

3.1 Revisiting the Loss Error

To motivate our proposed approach, we first revisit the loss error ϵ_i in Equation 8, which approximates the (detrimental) increase in the network’s task loss, introduced by quantizing weight w_i . This error ϵ_i has been used as a heuristic in multiple previous works (LeCun et al., 1989; Hassibi et al., 1993; Singh and Alistarh, 2020; Frantar and Alistarh, 2022) for choosing the next best weight i to prune or quantize. It has been shown to be a highly informative metric for measuring the impact of quantization.

By examining Equation 8, one finds that the loss error ϵ_i is proportional to the square of weight quantization error and inversely proportional to the di-

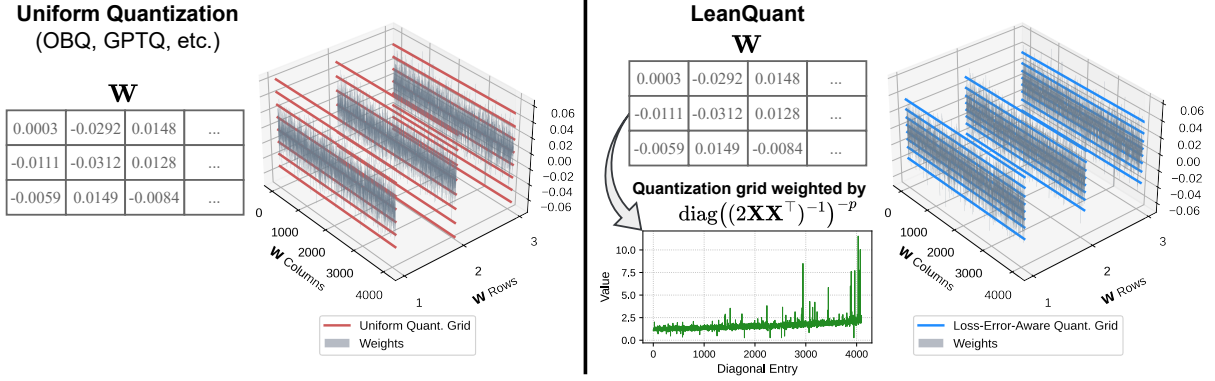


Figure 2: The uniform quantization grid (left), used by methods such as OBQ and GPTQ, compared to the loss-error-aware quantization grid (right), employed by LeanQuant. The results show the 3-bit quantization of the first MLP-Up linear layer in LLaMA-2-7b.

agonal entry of the inverse Hessian, i.e.,

$$\epsilon_i \propto (\text{quant}(w_i) - w_i)^2 \text{ and } \epsilon_i \propto \frac{1}{\mathbf{H}_{i,i}^{-1}} \quad (10)$$

Hence, we further examine the empirical distribution of $\frac{1}{\text{diag}(\mathbf{H}^{-1})}$, to which the loss error row vector ϵ is proportional. We obtain the empirical distributions on layers of LLaMA-2-7b (Touvron et al., 2023b) with 128 sequences of length 2048 tokens from the C4 dataset (Raffel et al., 2020), and compute the inverse Hessian as $\mathbf{H}^{-1} = (2\mathbf{X}\mathbf{X}^\top)^{-1}$ where \mathbf{X} is the layer input matrix. As shown in Figure 1, The majority of the inverse diagonals are concentrated in low-magnitude regions, with a few outliers having high magnitudes. Quantizing the weights corresponding to these outliers can lead to high loss errors if these weights are not well-aligned with the quantization grid. Preserving the quantized precision of the weights corresponding to these inverse-diagonal outliers is especially important because the loss error increases quadratically with their quantization error (Equation 10). Iterative weight-update-based quantization approaches (OBQ, GPTQ, etc.) employ uniform quantization grid, which is suboptimal for preserving the quantized precision of the inverse-diagonal outliers, leading to high loss error and model quality degradation. Our idea is to shape the quantization grid to minimize the loss error ϵ .

3.2 Loss-Error-Aware Network Quantization

The grid lines in a uniform quantization grid are evenly spaced, making it ineffective for preserving the quantized precision of weights associated with inverse-diagonal outliers. To mitigate this issue, we adopt a non-uniform loss-error-aware quantization

grid, which is well-aligned with weights that can potentially cause high loss errors. Concretely, we learn the set of grid lines \mathcal{G} for b -bit quantization through the following objective,

$$\arg \min_{\mathcal{G}: |\mathcal{G}|=2^b} \sum_i (\mathbf{H}_{i,i}^{-1})^{-p} |\text{quant}(w_i, \mathcal{G}) - w_i|^2 \quad (11)$$

where $\text{quant}(w_i, \mathcal{G}) = \arg \min_{g \in \mathcal{G}} |g - w_i|$ rounds w_i to the nearest grid line in \mathcal{G} and p is a hyperparameter for weighing the importance of preserving quantized precision of outliers. We leverage k-means++ (Arthur et al., 2007) to optimize the objective. After the quantization grid \mathcal{G} has been established, the weights are iteratively quantized to the nearest grid line in \mathcal{G} . Our proposed loss-error-aware quantization grid can integrate with any OBQ-based approaches to reduce the impact of quantization on the task loss. We propose LeanQuant-Exact (Algorithm 2 in the Appendix), which integrates loss-error-aware quantization grid with OBQ (Frantar and Alistarh, 2022), for quantizing million-parameter language models. For efficiently and accurately quantizing billion-parameter LLMs, we propose LeanQuant (Algorithm 1), which integrates loss-error-aware quantization grid with GPTQ (Frantar et al., 2022). An illustrative comparison between uniform quantization and LeanQuant is shown in Figure 2.

The goal of LeanQuant is to prevent drastic increase to the task loss by shaping the quantization grid \mathcal{G} to better preserve precision of the weights corresponding to the outlier inverse diagonals. As a consequence of the learning objective in Equation 11, a weight w_i with a larger inverse diagonal $\frac{1}{\mathbf{H}_{i,i}^{-1}}$ will tend to have less quantization error $|\text{quant}(w_i, \mathcal{G}) - w_i|$. However, since the weights

will shift during the iterative quantization process and the quantization grid is fixed beforehand, one potential problem arises that the quantization grid is no longer well-aligned with the outliers after certain iterations. Fortunately, this is not a problem in practice. The loss-error-awareness of LeanQuant grids prevents large values of $\frac{|\text{quant}(w_i, \mathcal{G})|}{\mathbf{H}_{i,i}^{-1}}$ from occurring, hence the weights do not shift by much during iterations as there are few high-norm weight perturbations δ_i . Furthermore, no new inverse-diagonal outliers will arise during the iterative quantization process, since the remaining inverse diagonals only decrease in magnitude towards zero after each column and row removal (Equation 9).

The parameter p balances the precision preservation of inverse-diagonal outliers and that of non-outliers. Higher values of p prioritizes the precision preservation of outliers more, while $p = 0$ prioritizes the preservation of all weights equally. We recommend the following values of p for b -bit quantization,

$$p = \begin{cases} 2.5 & \text{for } b = 4 \\ 3 & \text{for } b = 3 \\ 3.5 & \text{for } b = 2 \end{cases} \quad (12)$$

These recommendations are derived from a parameter search for the best p on different-sized LLaMA models (Touvron et al., 2023a), with the results presented in Table 8 in the Appendix. Quantization under lower bit widths requires higher values of p . We hypothesize that this is due to quantized precision of diagonal outliers having a stronger impact on the model quality in lower bit-width regions.

3.3 Storage, Learning and Computational Overheads

Storage Overhead Due to the non-uniformity of quantization grids, LeanQuant grid lines are stored in 16-bit floating-point (FP16) numbers. This introduces a slight storage overhead for quantized models when compared to a uniform quantization grid, in which only the zero-point and the scaling factor are stored in FP16. Fortunately, this overhead is negligible to the overall size of the quantized model, as it only introduces 0.01–0.05 bits per weight (BPW) for 7b–70b LLaMA models under 2/3/4-bit quantization. The detailed calculations for BPW are presented in Section B in the Appendix.

Learning Overhead Quantizing billions of parameters in LLMs efficiently is a significant challenge. Our method can easily scale to very large

Algorithm 1 LeanQuant for LLMs

Input: weight matrix $\mathbf{W} \in \mathbb{R}^{r \times c}$, sample input matrix \mathbf{X} , bit width b , block size B , hyperparameter p
Output: Quantized matrix $\hat{\mathbf{W}}$

- 1: $\hat{\mathbf{W}} \leftarrow \mathbf{0}_{r \times c}$
- 2: $\mathbf{E} \leftarrow \mathbf{0}_{r \times B}$
- 3: $\mathbf{H} \leftarrow 2\mathbf{X}\mathbf{X}^\top$
- 4: $\mathbf{H}^{-1} \leftarrow \text{Cholesky}\left(\left[\mathbf{H} + \frac{\text{avg}(\text{diag}(\mathbf{H}))}{100} \cdot \mathbf{I}\right]^{-1}\right)$
 \triangleright Apply damping, inversion, and Cholesky decomp.
- 5: $\mathcal{G}_k \leftarrow \arg \min_{\mathcal{G}: |\mathcal{G}|=2^b} (\text{diag}(\mathbf{H}^{-1})^{-p})^\top |\text{quant}(\mathbf{W}_{k,:}, \mathcal{G}) - \mathbf{W}_{k,:}|^2$ **forall** $k \in \{0, \dots, r-1\}$
 \triangleright Apply k-means++ to learn quantization grids
- 6: **for** $i \leftarrow 0, B, 2B, \dots$ **do** \triangleright Block-wise quantization
- 7: **for** $j \leftarrow i, \dots, i+B-1$ **do**
- 8: $\mathbf{W}_{k,j} \leftarrow \text{quant}(\mathbf{W}_{k,j}, \mathcal{G}_k)$ **forall** $k \in \{0, \dots, r-1\}$
 \triangleright Quantize each row to its corresponding grid
- 9: $\mathbf{E}_{:,j-1} \leftarrow \frac{\mathbf{W}_{:,j} - \hat{\mathbf{W}}_{:,j}}{\mathbf{H}_{j,j}^{-1}}$
- 10: $\mathbf{W}_{:,j:(i+B)} \leftarrow \mathbf{W}_{:,j:(i+B)} - \mathbf{E}_{:,j-i} \cdot \mathbf{H}_{j,j:(i+B)}^{-1}$
- 11: **end for**
- 12: $\mathbf{W}_{:,i:(i+B)} \leftarrow \mathbf{W}_{:,i:(i+B)} - \mathbf{E} \cdot \mathbf{H}_{i:(i+B), i:(i+B)}^{-1}$
- 13: **end for**
- 14: **return** $\hat{\mathbf{W}}$

language models without requiring excessive hardware. In our experiments, we are able to quantize LLaMA-2-70b (Touvron et al., 2023b) in under 6 hours using a single V100-32GB GPU. Compared to OBQ or GPTQ, LeanQuant requires no additional information such as loss gradient or extra calibration samples. LeanQuant learns the quantization grids through k-means++ (Arthur et al., 2007), which is computationally lightweight compared to the iterative quantization process. The quantization time costs are presented in Table 6 in the Appendix.

Inference Efficiency We leverage GPU kernel fusion for efficient inference of LeanQuant models. The matrix multiplication for each quantized layer is performed on-chip by fusing the kernels for dequantization and matrix multiplication. Each quantization grid is stored in a lookup table, which is highly compact (16 FP16 numbers for a 4-bit grid) and does not negatively impact the inference efficiency. We compare the decoding performance of LeanQuant with unquantized models in Table 5.

4 Experiments

In this section, we perform extensive experiments to validate the effectiveness of our proposed approach LeanQuant for quantizing language models against competitive baselines.

Method	BPW	LLaMA (version-size) on WikiText-2							LLaMA (version-size) on C4						
		1-7b	1-13b	1-30b	1-65b	2-7b	2-13b	2-70b	1-7b	1-13b	1-30b	1-65b	2-7b	2-13b	2-70b
FP16	16	5.58	5.09	4.10	3.53	5.47	4.88	3.31	7.08	6.61	5.98	5.62	6.97	6.46	5.52
GPTQ-g128	4.24-4.25	5.85	5.20	4.23	3.65	5.61	4.98	3.42	7.21	6.69	6.06	5.69	7.12	6.56	5.58
AWQ-g128	4.24-4.25	5.81	5.20	4.21	3.62	5.62	4.97	-	7.21	6.70	6.05	5.68	7.13	6.56	-
GPTQ	4.00	6.13	5.40	4.48	3.83	5.83	5.13	3.58	7.43	6.84	6.20	5.80	7.37	6.70	5.67
AWQ	4.00	6.08	5.34	4.39	3.76	6.15	5.12	-	7.52	6.86	6.17	5.77	7.68	6.74	-
OmniQuant	4.00	5.86	5.21	4.25	3.71	5.74	5.02	3.47	7.34	6.76	6.11	5.73	7.35	6.65	5.65
LeanQuant	4.04-4.05	5.81	5.19	4.21	3.65	5.62	5.00	3.42	7.21	6.70	6.06	5.69	7.13	6.57	5.58
GPTQ-g128	3.24-3.25	6.55	5.62	4.80	4.17	6.29	5.42	3.85	7.85	7.10	6.47	6.00	7.89	7.00	5.85
AWQ-g128	3.24-3.25	6.46	5.51	4.63	3.99	6.24	5.32	-	7.92	7.07	6.37	5.94	7.84	6.94	-
GPTQ	3.00	8.06	6.76	5.84	5.06	8.37	6.44	4.82	9.49	8.16	7.29	6.71	9.81	8.02	6.57
AWQ	3.00	11.88	7.45	10.07	5.21	24.00	10.45	-	13.26	9.13	12.67	7.11	23.85	13.07	-
OmniQuant	3.00	6.49	5.68	4.74	4.04	6.58	5.58	3.92	8.19	7.32	6.57	6.07	8.65	7.44	6.06
LeanQuant	3.02	6.37	5.60	4.71	4.08	6.30	5.40	3.80	7.79	7.05	6.42	5.99	7.80	6.98	5.83
GPTQ-g128	2.24-2.25	44.01	15.60	10.92	9.51	36.77	28.14	NaN	27.71	15.29	11.93	11.99	33.70	20.97	NaN
AWQ-g128	2.24-2.25	>10 ³	>10 ³	>10 ³	>10 ³	>10 ³	>10 ³	-	>10 ³	>10 ³	>10 ³	>10 ³	>10 ³	>10 ³	-
GPTQ	2.00	>10 ³	>10 ³	499.75	55.91	>10 ³	>10 ³	77.95	689.13	>10 ³	169.80	40.58	NaN	323.12	48.82
OmniQuant	2.00	15.47	13.21	8.71	7.58	37.37	17.21	7.81	24.89	18.31	13.89	10.77	90.64	26.76	12.28
LeanQuant	2.01	15.65	9.64	7.34	6.80	14.98	10.32	6.22	17.62	10.93	8.91	8.54	17.89	11.73	7.96

Table 1: Perplexity of LLaMA models under different quantization methods on WikiText-2 and C4. The results of GPTQ, AWQ, and OmniQuant are from Shao et al. (2024). LeanQuant mostly outperforms baselines under similar bit widths.

4.1 Experimental Setup

We perform two distinct sets of experiments for measuring model quality: evaluations of LeanQuant on quantizing billion-parameter LLMs, and evaluations of LeanQuant-Exact on quantizing million-parameter BERT models.

LLM Experiments We compare the quality of quantized LLMs under different quantization approaches. The LLMs considered are LLaMA-1 (7/13/30/65b) (Touvron et al., 2023a) and LLaMA-2 (7/13/70b) (Touvron et al., 2023b), and the quantization baseline methods considered are 1. GPTQ (Frantar et al., 2022) (no grouping and with a group size of 128), 2. AWQ (Lin et al., 2024) (no grouping and with a group size of 128), 3. OmniQuant (Shao et al., 2024), 4. QUIP (Chee et al., 2024). We evaluate model quality through the perplexity score on the datasets WikiText-2 (Merity et al., 2016) and C4 (Raffel et al., 2020), and through the zero-shot accuracy on 4 benchmarks: 1. Arc Easy (ArcE) (Clark et al., 2018), 2. Arc Challenge (ArcC) (Clark et al., 2018), 3. PIQA (Bisk et al., 2020), 4. WinoGrande (WG) (Sakaguchi et al., 2021). We follow the GPTQ settings (Frantar et al., 2022) for measuring perplexity, where sequences from the test set are concatenated into 128 sequences of length 2048 tokens for perplexity testing, and use lm-eval (Gao et al., 2023) for benchmarking zero-

shot accuracy. For LeanQuant, all models are calibrated on a set of 128 sequences of length 2048 tokens from the training set of C4, and quantized with a single V100-32GB GPU and an Intel Xeon E5-2699A v4 CPU. The hyperparameter p is set according to Equation 12.

BERT Experiments We compare the performance of BERT models (Devlin et al., 2018), quantized with OBQ (Frantar and Alistarh, 2022) and LeanQuant, on the SQuAD dataset (Rajpurkar et al., 2016). We quantize the 12-layer BERT-base and the 3-layer BERT-3 variant from Kurtic et al. (2022) to 3 and 4 bits. OBQ and LeanQuant-Exact are calibrated using 1024 samples from the training set, and the F1 score is reported on the test set.

4.2 Results

For the LLM evaluations, the perplexity on WikiText-2 and C4 are presented in Table 1, and the zero-shot accuracy on 4 benchmarks are presented in Table 2. For evaluations on BERT models, the F1 scores are presented in Table 3. Bits per weight (BPW) are reported for each method for a fair comparison, and their calculations are presented in Section B in the Appendix.

In terms of perplexity, LeanQuant outperforms competitive baselines at similar bit widths in most cases, with particularly significant performance

	Method	BPW	ArcC	ArcE	PIQA	WG	Avg
LLaMA-2-7b	FP16	16	40.0	69.3	78.5	67.3	63.8
	OmniQuant	4.00	37.9	67.8	77.1	67.0	62.5
	LeanQuant	4.05	38.6	69.2	77.4	67.5	63.2
	OmniQuant	3.00	35.3	62.6	73.6	63.6	58.8
	LeanQuant	3.02	37.7	68.3	76.5	67.5	62.5
	QUIP	2.00	19.4	26.0	54.6	51.8	38.0
	OmniQuant	2.00	21.6	35.2	57.5	51.5	41.5
	LeanQuant	2.01	24.7	44.2	65.4	57.4	47.9
	FP16	16	45.6	73.3	78.7	69.6	66.8
	QUIP	4.00	44.9	73.3	79.0	69.7	66.7
LLaMA-2-13b	OmniQuant	4.00	43.1	70.2	78.4	67.8	64.9
	LeanQuant	4.04	44.4	73.3	78.5	69.7	66.5
	QUIP	3.00	41.5	70.4	76.9	69.9	64.7
	OmniQuant	3.00	42.0	69.0	77.7	65.9	63.7
	LeanQuant	3.02	41.8	72.1	77.1	69.9	65.2
	QUIP	2.00	23.5	45.2	62.0	52.8	45.9
	OmniQuant	2.00	23.0	44.4	62.6	52.6	45.7
	LeanQuant	2.01	28.2	56.7	70.6	60.7	54.0
	FP16	16	51.1	77.7	81.1	77.0	71.7
	QUIP	4.00	47.0	74.3	80.3	76.0	69.4
LLaMA-2-70b	OmniQuant	4.00	49.8	77.9	80.7	75.8	71.1
	LeanQuant	4.04	50.6	77.7	81.0	77.0	71.6
	QUIP	3.00	46.3	73.2	80.0	74.6	68.5
	OmniQuant	3.00	47.6	75.7	79.7	73.5	69.1
	LeanQuant	3.02	48.9	76.7	80.2	77.0	70.7
	QUIP	2.00	34.0	62.2	74.8	67.5	59.6
	OmniQuant	2.00	28.7	55.4	68.8	53.2	51.5
	LeanQuant	2.01	42.1	71.6	77.9	74.8	66.6

Table 2: Zero-shot accuracy of quantized LLaMA-2 models on 4 benchmarks. The results of QUIP and OmniQuant are from Tseng et al. (2024). LeanQuant outperforms baselines under similar bit widths in most cases.

gains in 2-bit quantization. Compared to grouped GPTQ and AWQ, LeanQuant performs similarly in 3/4-bit quantization despite using lower BPW, and significantly outperforms them in 2-bit quantization. In terms of the zero-shot accuracy results, LeanQuant mostly outperforms baselines in 3/4-bit quantization, and performs significantly better (6.4%–15.1% improvement) in 2-bit. On BERT models, LeanQuant-Exact consistently outperforms OBQ in maintaining model quality.

4.3 Ablation Study

We perform an ablation study to answer the following questions.

Q1: Does LeanQuant effectively reduce the loss error ϵ compared to GPTQ? Yes, the loss-error-aware quantization grids of LeanQuant effectively reduce loss errors ϵ compared to GPTQ.

Method	BPW	BERT-3	BERT
FP32	32	84.66	88.53
OBQ	4.03	84.40	87.96
LeanQuant-Exact	4.13	84.58	88.49
OBQ	3.03	83.47	84.72
LeanQuant-Exact	3.06	84.20	86.21

Table 3: F1 scores on SQuAD of BERT models quantized using OBQ and LeanQuant-Exact. LeanQuant-Exact outperforms OBQ in maintaining model quality.

	Method	BPW	Perplexity	
			WikiText-2	C4
LLaMA-2-7b	FP16	16	5.47	6.97
	GPTQ+Non-uniform Grid	4.05	5.68	7.16
	LeanQuant	4.05	5.62	7.13
	GPTQ+Non-uniform Grid	3.02	6.69	8.19
	LeanQuant	3.02	6.30	7.80
	GPTQ+Non-uniform Grid	2.01	NaN	69.22
	LeanQuant	2.01	14.98	17.89
	LLaMA-2-13b	FP16	16	4.88
GPTQ+Non-uniform Grid		4.04	5.02	6.57
LeanQuant		4.04	5.00	6.57
GPTQ+Non-uniform Grid		3.02	5.72	7.21
LeanQuant		3.02	5.40	6.98
GPTQ+Non-uniform Grid		2.01	179.29	212.46
LeanQuant		2.01	10.32	11.73

Table 4: Comparison of LeanQuant and GPTQ with uninformed non-uniform quantization grids, on the perplexity of LLaMA-2 models on WikiText-2 and C4.

Figure 3 presents the layer-wise sum of loss errors ϵ for 4/3/2-bit LLaMA-2 models quantized using GPTQ and LeanQuant. The sum of loss errors are computed as Equation 8, summed over all weights for each linear layer. LeanQuant effectively reduces loss error compared to GPTQ, especially in lower bit-width regions.

Q2: How does the loss-error-aware quantization grid compare with an uninformed non-uniform quantization grid? A loss-error-aware quantization grid maintains model quality significantly better than an uninformed counterpart. Table 4 presents the perplexity results of LeanQuant and GPTQ with uninformed non-uniform quantization grids. The uninformed non-uniform quantization grids are learned using Equation 11 with $p = 0$, which removes the diagonal inverse Hessians as weighting factors and aims to preserve all weights equally. Loss-error-aware quantization grids consistently outperforms uninformed non-uniform grids, particularly in lower bit widths.

Q3: Is LeanQuant sensitive to the hyperparameter p ? We found LeanQuant to be not very

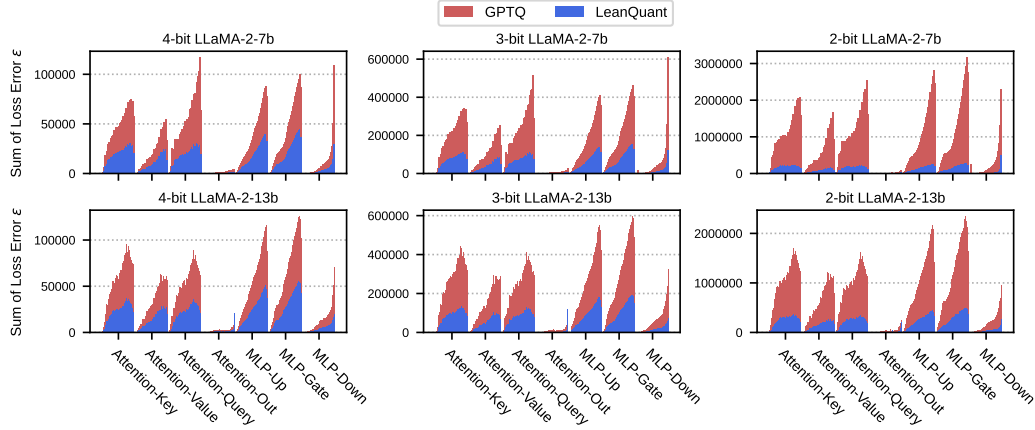


Figure 3: The sum of loss error ϵ of GPTQ and LeanQuant (overlaid on GPTQ) for each layer in 4/3/2-bit quantized LLaMA-2 models. LeanQuant achieves significantly lower loss errors than GPTQ, especially in lower bit-width regions.

	Method	Time Cost	Peak VRAM
LLaMA-2-7b	FP16	4.872s	25970 MB
	4-bit LeanQuant	1.963s	4528 MB
	3-bit LeanQuant	1.553s	3667 MB
LLaMA-2-13b	FP16	-	OOM
	4-bit LeanQuant	3.193s	7901 MB
	3-bit LeanQuant	2.420s	6385 MB

Table 5: Inference time cost and peak GPU RAM usage of decoding 128 tokens for LeanQuant and unquantized LLaMA-2 models.

sensitive to p . The results of a parameter search over p are presented in Table 8 in the Appendix.

4.4 Inference Efficiency

We compare the inference efficiency of LeanQuant with unquantized FP16 models. We perform inference with LLaMA-2 models to generate 128 tokens using a V100 32GB GPU. Our implementation is based on HuggingFace Transformers (Wolf et al., 2019) and the CUDA time and peak GPU RAM usage is recorded using the PyTorch profiler (Paszke et al., 2019). The results are presented in Table 5. On LLaMA-2-7b, LeanQuant achieves $2.48\times$ and $3.14\times$ speedup over the unquantized model with 4-bit and 3-bit quantization, respectively. The unquantized LLaMA-2-13b model exceeds the memory limits of a 32GB GPU, while the 4-bit and 3-bit LeanQuant models fit comfortably within this constraint.

5 Related Works

Optimal Brain Damage (LeCun et al., 1989) introduced a saliency-score-based iterative pruning

algorithm for neural networks, and Optimal Brain Surgeon (Hassibi and Stork, 1992; Hassibi et al., 1993) extended it to apply a weight update to compensate for the introduced error in each iteration. These methods inspired a number of works on network pruning (Guo et al., 2016; Singh and Alistarh, 2020; Yu et al., 2022) and weight quantization (Li et al., 2021; Frantar and Alistarh, 2022; Frantar et al., 2022).

LLM inference is computationally and memory demanding. Existing works accelerate LLM inference and reduce memory requirements through weight quantization (Dettmers et al., 2022; Lin et al., 2024; Frantar et al., 2022; Chee et al., 2024; Kim et al., 2023; Shao et al., 2024), weight pruning (Frantar and Alistarh, 2023; Ashkboos et al., 2024), weight-activation quantization (Xiao et al., 2023), KV cache quantization (Zhang et al., 2024a), offloading (Sheng et al., 2023), hardware-aware algorithmic designs (Dao et al., 2022; Zhang et al., 2024b), etc.

6 Conclusion

In this work, we pinpoint the uniform quantization grids as a limitation of the Optimal Brain Quantization (OBQ) framework, which causes large errors in the network’s task loss. To address this issue, we propose LeanQuant, which shapes quantization grids to better preserve the precision of inverse diagonal outliers, leading to significantly lower loss errors and better model quality. Extensive empirical evaluations reveal that our proposed approach quantizes LLMs efficiently and accurately, compares favorably to existing competitive baselines, and effectively speeds up model inference.

Limitations

Quantization is a form of lossy compression that impacts model quality. While we evaluate the quality of quantized models through perplexity and accuracy metrics, it remains unclear how our proposed quantization approach affects various aspects of models such as generation quality, interpretability, harmfulness, truthfulness, fairness, and adversarial robustness.

References

- David Arthur, Sergei Vassilvitskii, et al. 2007. k-means++: The advantages of careful seeding. In *Soda*, volume 7, pages 1027–1035.
- Saleh Ashkboos, Maximilian L Croci, Marcelo Genari do Nascimento, Torsten Hoeftler, and James Hensman. 2024. Slicept: Compress large language models by deleting rows and columns. *arXiv preprint arXiv:2401.15024*.
- Yonatan Bisk, Rowan Zellers, Jianfeng Gao, Yejin Choi, et al. 2020. Piqa: Reasoning about physical commonsense in natural language. In *Proceedings of the AAAI conference on artificial intelligence*, volume 34, pages 7432–7439.
- Jerry Chee, Yaohui Cai, Volodymyr Kuleshov, and Christopher M De Sa. 2024. Quip: 2-bit quantization of large language models with guarantees. *Advances in Neural Information Processing Systems*, 36.
- Lingjiao Chen, Matei Zaharia, and James Zou. 2023. Frugalpt: How to use large language models while reducing cost and improving performance. *arXiv preprint arXiv:2305.05176*.
- Peter Clark, Isaac Cowhey, Oren Etzioni, Tushar Khot, Ashish Sabharwal, Carissa Schoenick, and Oyvind Tafjord. 2018. Think you have solved question answering? try arc, the ai2 reasoning challenge. *arXiv preprint arXiv:1803.05457*.
- Tri Dao, Dan Fu, Stefano Ermon, Atri Rudra, and Christopher Ré. 2022. Flashattention: Fast and memory-efficient exact attention with io-awareness. *Advances in Neural Information Processing Systems*, 35:16344–16359.
- Tim Dettmers, Mike Lewis, Younes Belkada, and Luke Zettlemoyer. 2022. Gpt3. int8 (): 8-bit matrix multiplication for transformers at scale. *Advances in Neural Information Processing Systems*, 35:30318–30332.
- Jacob Devlin, Ming-Wei Chang, Kenton Lee, and Kristina Toutanova. 2018. Bert: Pre-training of deep bidirectional transformers for language understanding. *arXiv preprint arXiv:1810.04805*.
- Elias Frantar and Dan Alistarh. 2022. Optimal brain compression: A framework for accurate post-training quantization and pruning. *Advances in Neural Information Processing Systems*, 35:4475–4488.
- Elias Frantar and Dan Alistarh. 2023. Sparsegpt: Massive language models can be accurately pruned in one-shot. In *International Conference on Machine Learning*, pages 10323–10337. PMLR.
- Elias Frantar, Saleh Ashkboos, Torsten Hoeftler, and Dan Alistarh. 2022. Gptq: Accurate post-training quantization for generative pre-trained transformers. *arXiv preprint arXiv:2210.17323*.
- Leo Gao, Jonathan Tow, Baber Abbasi, Stella Biderman, Sid Black, Anthony DiPofi, Charles Foster, Laurence Golding, Jeffrey Hsu, Alain Le Noac’h, Haonan Li, Kyle McDonell, Niklas Muennighoff, Chris Ociepa, Jason Phang, Laria Reynolds, Hailey Schoelkopf, Aviya Skowron, Lintang Sutawika, Eric Tang, Anish Thite, Ben Wang, Kevin Wang, and Andy Zou. 2023. [A framework for few-shot language model evaluation](#).
- Yiwen Guo, Anbang Yao, and Yurong Chen. 2016. Dynamic network surgery for efficient dnns. *Advances in neural information processing systems*, 29.
- Babak Hassibi and David Stork. 1992. Second order derivatives for network pruning: Optimal brain surgeon. *Advances in neural information processing systems*, 5.
- Babak Hassibi, David G Stork, and Gregory J Wolff. 1993. Optimal brain surgeon and general network pruning. In *IEEE international conference on neural networks*, pages 293–299. IEEE.
- Jean Kaddour, Joshua Harris, Maximilian Mozes, Herbie Bradley, Roberta Raileanu, and Robert McHardy. 2023. Challenges and applications of large language models. *arXiv preprint arXiv:2307.10169*.
- Enkelejda Kasneci, Kathrin Seßler, Stefan Küchemann, Maria Bannert, Daryna Dementieva, Frank Fischer, Urs Gasser, Georg Groh, Stephan Günnemann, Eyke Hüllermeier, et al. 2023. Chatgpt for good? on opportunities and challenges of large language models for education. *Learning and individual differences*, 103:102274.
- Sehoon Kim, Coleman Hooper, Amir Gholami, Zhen Dong, Xiuyu Li, Sheng Shen, Michael W Mahoney, and Kurt Keutzer. 2023. Squeezellm: Dense-and-sparse quantization. *arXiv preprint arXiv:2306.07629*.
- Takeshi Kojima, Shixiang Shane Gu, Machel Reid, Yutaka Matsuo, and Yusuke Iwasawa. 2022. Large language models are zero-shot reasoners. *Advances in neural information processing systems*, 35:22199–22213.
- Raghuraman Krishnamoorthi. 2018. Quantizing deep convolutional networks for efficient inference: A whitepaper. *arXiv preprint arXiv:1806.08342*.

- Eldar Kurtic, Daniel Campos, Tuan Nguyen, Elias Frantar, Mark Kurtz, Benjamin Fineran, Michael Goin, and Dan Alistarh. 2022. The optimal bert surgeon: Scalable and accurate second-order pruning for large language models. *arXiv preprint arXiv:2203.07259*.
- Yann LeCun, John Denker, and Sara Solla. 1989. Optimal brain damage. *Advances in neural information processing systems*, 2.
- Juhang Li, Ruihao Gong, Xu Tan, Yang Yang, Peng Hu, Qi Zhang, Fengwei Yu, Wei Wang, and Shi Gu. 2021. Brecq: Pushing the limit of post-training quantization by block reconstruction. *arXiv preprint arXiv:2102.05426*.
- Ji Lin, Jiaming Tang, Haotian Tang, Shang Yang, Weiming Chen, Wei-Chen Wang, Guangxuan Xiao, Xingyu Dang, Chuang Gan, and Song Han. 2024. Awq: Activation-aware weight quantization for on-device llm compression and acceleration. *Proceedings of Machine Learning and Systems*, 6:87–100.
- Stephen Merity, Caiming Xiong, James Bradbury, and Richard Socher. 2016. Pointer sentinel mixture models. *arXiv preprint arXiv:1609.07843*.
- Markus Nagel, Rana Ali Amjad, Mart Van Baalen, Christos Louizos, and Tijmen Blankevoort. 2020. Up or down? adaptive rounding for post-training quantization. In *International Conference on Machine Learning*, pages 7197–7206. PMLR.
- Adam Paszke, Sam Gross, Francisco Massa, Adam Lerer, James Bradbury, Gregory Chanan, Trevor Killeen, Zeming Lin, Natalia Gimelshein, Luca Antiga, et al. 2019. Pytorch: An imperative style, high-performance deep learning library. *Advances in neural information processing systems*, 32.
- Colin Raffel, Noam Shazeer, Adam Roberts, Katherine Lee, Sharan Narang, Michael Matena, Yanqi Zhou, Wei Li, and Peter J Liu. 2020. Exploring the limits of transfer learning with a unified text-to-text transformer. *Journal of machine learning research*, 21(140):1–67.
- Pranav Rajpurkar, Jian Zhang, Konstantin Lopyrev, and Percy Liang. 2016. Squad: 100,000+ questions for machine comprehension of text. *arXiv preprint arXiv:1606.05250*.
- Keisuke Sakaguchi, Ronan Le Bras, Chandra Bhagavatula, and Yejin Choi. 2021. Winogrande: An adversarial winograd schema challenge at scale. *Communications of the ACM*, 64(9):99–106.
- Wenqi Shao, Mengzhao Chen, Zhaoyang Zhang, Peng Xu, Lirui Zhao, Zhiqian Li, Kaipeng Zhang, Peng Gao, Yu Qiao, and Ping Luo. 2024. [Omniquant: Omnidirectionally calibrated quantization for large language models](#). In *The Twelfth International Conference on Learning Representations*.
- Ying Sheng, Lianmin Zheng, Binhang Yuan, Zhuohan Li, Max Ryabinin, Beidi Chen, Percy Liang, Christopher Ré, Ion Stoica, and Ce Zhang. 2023. Flexgen: High-throughput generative inference of large language models with a single gpu. In *International Conference on Machine Learning*, pages 31094–31116. PMLR.
- Sidak Pal Singh and Dan Alistarh. 2020. Woodfisher: Efficient second-order approximation for neural network compression. *Advances in Neural Information Processing Systems*, 33:18098–18109.
- Hugo Touvron, Thibaut Lavril, Gautier Izacard, Xavier Martinet, Marie-Anne Lachaux, Timothée Lacroix, Baptiste Rozière, Naman Goyal, Eric Hambro, Faisal Azhar, et al. 2023a. Llama: Open and efficient foundation language models. *arXiv preprint arXiv:2302.13971*.
- Hugo Touvron, Louis Martin, Kevin Stone, Peter Albert, Amjad Almahairi, Yasmine Babaei, Nikolay Bashlykov, Soumya Batra, Prajjwal Bhargava, Shruti Bhosale, et al. 2023b. Llama 2: Open foundation and fine-tuned chat models. *arXiv preprint arXiv:2307.09288*.
- Albert Tseng, Jerry Chee, Qingyao Sun, Volodymyr Kuleshov, and Christopher De Sa. 2024. Quip#: Even better llm quantization with hadamard incoherence and lattice codebooks. *arXiv preprint arXiv:2402.04396*.
- Jason Wei, Xuezhi Wang, Dale Schuurmans, Maarten Bosma, Fei Xia, Ed Chi, Quoc V Le, Denny Zhou, et al. 2022. Chain-of-thought prompting elicits reasoning in large language models. *Advances in neural information processing systems*, 35:24824–24837.
- Thomas Wolf, Lysandre Debut, Victor Sanh, Julien Chaumond, Clement Delangue, Anthony Moi, Pierric Cistac, Tim Rault, Rémi Louf, Morgan Funtowicz, et al. 2019. Huggingface’s transformers: State-of-the-art natural language processing. *arXiv preprint arXiv:1910.03771*.
- Guangxuan Xiao, Ji Lin, Mickael Seznec, Hao Wu, Julien Demouth, and Song Han. 2023. Smoothquant: Accurate and efficient post-training quantization for large language models. In *International Conference on Machine Learning*, pages 38087–38099. PMLR.
- Xin Yu, Thiago Serra, Srikumar Ramalingam, and Shandian Zhe. 2022. The combinatorial brain surgeon: pruning weights that cancel one another in neural networks. In *International Conference on Machine Learning*, pages 25668–25683. PMLR.
- Tianyi Zhang, Jonah Yi, Zhaozhuo Xu, and Anshumali Shrivastava. 2024a. Kv cache is 1 bit per channel: Efficient large language model inference with coupled quantization. *arXiv preprint arXiv:2405.03917*.
- Tianyi Zhang, Jonah Wonkyu Yi, Bowen Yao, Zhaozhuo Xu, and Anshumali Shrivastava. 2024b. Nomad-attention: Efficient llm inference on cpus

through multiply-add-free attention. *arXiv preprint arXiv:2403.01273*.

Appendix

A LeanQuant-Exact

The pseudocode of LeanQuant-Exact for quantizing million-parameter networks is presented in Algorithm 2.

Algorithm 2 LeanQuant-Exact for Million-parameter Networks

Input: a row $\mathbf{w} \in \mathbb{R}^c$ in the weight matrix, sample input matrix \mathbf{X} , bit width b , hyperparameter p
Output: Quantized row $\hat{\mathbf{w}}$

- 1: $\hat{\mathbf{w}} \leftarrow \mathbf{0}_c$
- 2: $\mathbf{H}^{-1} \leftarrow (2\mathbf{X}\mathbf{X}^\top)^{-1}$
- 3: $\mathcal{G} \leftarrow \arg \min_{\mathcal{G}: |\mathcal{G}|=2^b} (\text{diag}(\mathbf{H}^{-1})^{-p})^\top |\text{quant}(\mathbf{w}, \mathcal{G}) - \mathbf{w}|^2$
 \triangleright Apply k-means++ to learn quantization grids
- 4: **for** $j \leftarrow 1, \dots, c$ **do**
- 5: $i \leftarrow \arg \min_i \frac{(\text{quant}(w_i, \mathcal{G}) - w_i)^2}{2\mathbf{H}_{i,i}^{-1}}$
- 6: $\hat{w}_i \leftarrow \text{quant}(w_i, \mathcal{G})$
- 7: $\mathbf{w} \leftarrow \mathbf{w} - \frac{\mathbf{H}_{:,i}^{-1}}{\mathbf{H}_{i,i}^{-1}} (w_i - \text{quant}(w_i, \mathcal{G}))$
- 8: $\mathbf{H}^{-1} \leftarrow \mathbf{H}^{-1} - \frac{\mathbf{H}_{:,i}^{-1} \mathbf{H}_{i,:}^{-1}}{\mathbf{H}_{i,i}^{-1}}$
- 9: **end for**
- 10: **return** $\hat{\mathbf{w}}$

B Bits Per Weight Calculations

This section describes how bits per weight (BPW) is calculated for LeanQuant. For b -bit quantization, LeanQuant stores a b -bit code for each individual parameter, and 2^b FP16 numbers (as the quantization grid) for each row of the weight matrix. We take LLaMA-2-7b as an example, which has 7 weight matrices in each of the 32 layers, and calculate its BPW under b -bit LeanQuant. The 7 weight matrix dimensions are ($d_{\text{row}} \times d_{\text{col}}$): $4096 \times 4096, 4096 \times 4096, 4096 \times 4096, 4096 \times 4096, 11008 \times 4096, 11008 \times 4096, 4096 \times 11008$. Therefore, the BPW per layer is

$$\underbrace{\frac{(4096 \times 5 + 11008 \times 2) \times 2^b}{4096 \times 4096 \times 4 + 11008 \times 4096 \times 3}}_{\text{bits for quantization grid}} \times 16 + \underbrace{b}_{\text{bits for codes}}$$

C Quantization Time Costs

The end-to-end quantization time costs for LeanQuant and LeanQuant-Exact for different sized models are presented in Table 6.

D Comparison with SqueezeLLM

We compare our proposed LeanQuant with SqueezeLLM, which is also a non-uniform quantization method for LLMs. The perplexity on

		Time to Quantize		
		4-bit	3-bit	2-bit
LeanQuant	LLaMA-2-7b	71 mins	54 mins	39 mins
	LLaMA-2-13b	97 mins	94 mins	77 mins
	LLaMA-2-70b	390 mins	329 mins	298 mins
LeanQuant-E	BERT-3	30 mins	30 mins	-
	BERT	126 mins	119 mins	-

Table 6: Time costs of LeanQuant and LeanQuant-Exact on different sized LLaMA and BERT models.

Method	BPW	LLaMA (version-size)			
		1-30b	1-65b	2-13b	2-70b
FP16	16	4.10	3.53	4.88	3.31
SqueezeLLM	4.04-4.05	4.22	3.76	4.99	3.41
LeanQuant	4.04-4.05	4.21	3.65	5.00	3.42
SqueezeLLM	3.02	4.66	4.05	5.36	3.77
LeanQuant	3.02	4.71	4.08	5.40	3.80
SqueezeLLM	2.01	-	-	41.02	9.44
LeanQuant	2.01	7.34	6.80	10.32	6.22

Table 7: Perplexity on WikiText-2, evaluated at length 2048 tokens, of LLaMA models quantized using SqueezeLLM and LeanQuant. The results of SqueezeLLM are from (Kim et al., 2023).

WikiText-2 of models quantized using these two methods are shown in Table 7. LeanQuant achieves comparable performance with SqueezeLLM at 3/4 bits, and achieves significantly better performance at 2 bits. Furthermore, the quantization process of SqueezeLLM requires computing the gradient on a sample dataset, which requires multiple GPUs for large models and is prone to overfitting. In comparison, LeanQuant does not use gradient information, and is able to quantize LLaMA-2-70b using a single V100-32GB GPU.

E Hyperparameter p

We perform a hyper-parameter search on LLaMA models (Touvron et al., 2023a,b) to identify the best p in Equation 11. The perplexity on WikiText-2 and C4 for different values of p are reported in Table 8. We found the following values of p generally work best for b -bit quantization,

$$p = \begin{cases} 2.5 & \text{for } b = 4 \\ 3 & \text{for } b = 3 \\ 3.5 & \text{for } b = 2 \end{cases} \quad (13)$$

The results on perplexity and accuracy reported in the main paper all follow the recommendations above.

F Artifact Licenses

In this section, we include the licenses for the artifacts used in the paper as follows.

1. LLaMA <https://ai.meta.com/llama/license/>
2. BERT <https://github.com/google-research/bert/blob/master/LICENSE>
3. Arc-Easy/Challenge <https://creativecommons.org/licenses/by-sa/4.0/>
4. WinoGrande <https://github.com/allenai/winogrande/blob/master/LICENSE>
5. SQuAD <https://creativecommons.org/licenses/by-sa/4.0/legalcode>

We use these artifacts strictly for evaluation purposes. Hence the use of existing artifacts in this work is consistent with their intended use.

G Potential Risks

We introduce no new models or datasets in this work. Therefore, we do not envision any additional potential risks from our work beyond those already associated with large language models.

Model	p	WikiText-2			C4		
		2-bit	3-bit	4-bit	2-bit	3-bit	4-bit
LLaMA-7b	1.0	126.65	6.41	5.84	81.66	7.90	7.24
	2.0	19.25	6.39	5.83	21.51	7.83	7.22
	2.5	20.25	6.39	5.81	22.80	7.81	7.21
	3.0	15.83	6.37	5.82	17.76	7.79	7.22
	3.5	15.65	6.34	5.83	17.62	7.76	7.21
	4.0	15.72	6.37	5.80	17.29	7.75	7.21
LLaMA-13b	1.0	16.33	5.56	5.19	17.20	7.08	6.70
	2.0	12.26	5.59	5.19	13.99	7.07	6.70
	2.5	10.04	-	5.19	11.98	-	6.70
	3.0	10.31	5.60	-	12.01	7.05	-
	3.5	9.64	5.61	5.20	10.93	7.05	6.70
	4.0	10.88	5.61	5.20	12.46	7.06	6.71
LLaMA-30b	1.0	12.82	4.79	-	17.58	6.47	-
	2.0	7.87	4.74	4.22	9.41	6.43	6.07
	2.5	7.63	4.69	4.21	9.43	6.42	6.06
	3.0	7.53	4.71	4.21	9.05	6.42	6.06
	3.5	7.34	4.71	4.21	8.91	6.41	6.06
	4.0	7.33	4.71	4.20	8.94	6.41	6.06
LLaMA-65b	1.0	99.43	4.22	3.66	128.63	6.06	5.69
	2.0	7.64	4.10	3.66	9.85	5.99	5.69
	2.5	6.99	4.11	3.65	8.91	5.99	5.69
	3.0	6.87	4.08	3.65	8.80	5.99	5.69
	3.5	6.80	4.10	3.67	8.54	5.99	5.69
	4.0	6.74	4.12	3.67	8.54	6.02	5.69
LLaMA-2-7b	1.0	266.80	6.39	5.62	-	7.95	7.13
	2.0	19.06	6.36	5.65	19.78	7.85	7.13
	2.5	15.64	6.28	5.62	15.76	7.81	7.13
	3.0	15.14	6.30	5.65	16.19	7.80	7.13
	3.5	14.98	6.26	5.66	17.89	7.79	7.14
	4.0	14.87	6.29	5.63	17.23	7.81	7.14
LLaMA-2-13b	1.0	31.59	5.49	5.00	41.91	7.21	6.57
	2.0	49.52	5.41	-	38.91	7.05	-
	2.5	10.42	5.40	5.00	12.67	6.99	6.57
	3.0	10.67	5.40	5.01	12.01	6.98	6.57
	3.5	10.23	5.42	5.00	11.73	6.99	6.58
	4.0	10.45	5.45	5.01	11.96	7.04	6.58
LLaMA-2-70b	2.5	-	-	3.42	-	-	5.58
	3.0	-	3.80	-	-	5.83	-
	3.5	6.22	-	-	7.96	-	-

Table 8: Perplexity of different models on WikiText-2 and C4 with varying p in Equation 11.